Microbiological Research 234 (2020) 126426

Contents lists available at ScienceDirect

Microbiological Research

journal homepage: www.elsevier.com/locate/micres

Identification of a gene encoding the last step of the L-rhamnose catabolic pathway in *Aspergillus niger* revealed the inducer of the pathway regulator

Tania Chroumpi[a], Maria Victoria Aguilar-Pontes[a,1], Mao Peng[a], Mei Wang[b], Anna Lipzen[b], Vivian Ng[b], Igor V. Grigoriev[b], Miia R. Mäkelä[c], Ronald P. de Vries[a,*]

[a] Fungal Physiology, Westerdijk Fungal Biodiversity Institute & Fungal Molecular Physiology, Utrecht University, Uppsalalaan 8, 3584 CT, Utrecht, the Netherlands
[b] DOE Joint Genome Institute, 2800 Mitchell Drive, Walnut Creek, CA 94598, United States
[c] Department of Microbiology, University of Helsinki, P.O. Box 56, Viikinkaari 9, Helsinki, Finland

ARTICLE INFO

Keywords:
L-rhamnose catabolic pathway
RhaR
Inducer
Pectinolytic enzymes
Gene regulation

ABSTRACT

In fungi, L-rhamnose (Rha) is converted *via* four enzymatic steps into pyruvate and L-lactaldehyde, which enter central carbon metabolism. In *Aspergillus niger*, only the genes involved in the first three steps of the Rha catabolic pathway have been identified and characterized, and the inducer of the pathway regulator RhaR remained unknown. In this study, we identified the gene (*lkaA*) involved in the conversion of L-2-keto-3-deoxyrhamnonate (L-KDR) into pyruvate and L-lactaldehyde, which is the last step of the Rha pathway. Deletion of *lkaA* resulted in impaired growth on L-rhamnose, and potentially in accumulation of L-KDR. Contrary to Δ*lraA*, Δ*lrlA* and Δ*lrdA*, the expression of the Rha-responsive genes that are under control of RhaR, were at the same levels in Δ*lkaA* and the reference strain, indicating the role of L-KDR as the inducer of the Rha pathway regulator.

1. Introduction

Pectin is one of the major components of plant cell walls. It represents a group of complex heteropolysaccharides with high diversity in their structure, which are composed of four structural elements: homogalacturonan (HGA), xylogalacturonan (XGA), rhamnogalacturonan I (RG-I) and rhamnogalacturonan II (RG-II) (Voragen et al., 2009). Due to the rather intricate composition of pectin, many fungi, including *Aspergillus niger,* produce a broad range of pectinolytic enzymes to efficiently degrade these polysaccharides (de Vries and Visser, 2001; Martens-Uzunova and Schaap, 2009; Benoit et al., 2012). These enzymes promote the decomposition of pectin into monosaccharides that the fungus can uptake and use as carbon source.

Although D-galacturonic acid (GalUA) is the predominant component of pectin, several other sugars are also part of its structure (Voragen et al., 2009). One of these is L-rhamnose (Rha), which is a hexose sugar abundantly present in both RG-I and RG-II. The backbone of RG-I is composed of alternating GalUA and Rha residues, while in RG-II, Rha is part of its side chains. Pectinolytic enzymes specifically involved in the release of Rha from pectin include exo- and endo-rhamnogalacturonase (EC 3.2.1.67), and α-L-rhamnosidase (EC 3.2.1.40), aided by rhamnogalacturonan galacturonohydrolase (exo-rhamnogalacturonase, EC 3.2.1.-), rhamnogalacturonan lyase (EC 4.2.2.-) and rhamnogalacturonan acetylesterase (EC 3.1.1.-) (de Vries et al., 2000; de Vries and Visser, 2001; Voragen et al., 2009).

After Rha is released, it is taken up in the fungal cell and converted through the fungal Rha catabolic pathway into pyruvate and L-lactaldehyde in four enzymatic steps (Fig. 1), which are sequentially catalyzed by L-rhamnose-1-dehydrogenase (LraA; EC 1.1.1.173), L-rhamnono-γ-lactonase (LrlA, formerly LraB; EC 3.1.1.65), L-rhamnonate

Abbreviations: CM, complete medium; 5-FOA, 5-fluoroorotic acid; GalUA, D-galacturonic acid; HGA, homogalacturonan; L-KDR, L-2-keto-3-deoxyrhamnonate; LraA, L-rhamnose-1-dehydrogenase; LrlA, L-rhamnono-γ-lactonase; LrdA, L-rhamnonate dehydratase; LkaA, L-2-keto-3-deoxyrhamnonate aldolase; NHEJ, non-homologous end-joining; RG-I, rhamnogalacturonan I; RG-II, rhamnogalacturonan II; Rha, L-rhamnose; RhaR, L-rhamnose responsive transcription factor; RhtA, L-rhamnose transporter; MM, minimal medium; XGA, xylogalacturonan

* Corresponding author.
E-mail address: r.devries@wi.knaw.nl (R.P. de Vries).
[1] Current address: Centre for Structural and Functional Genomics, Concordia University, 7141 Sherbrooke Street West, Montreal, Quebec, H4B1R6, Canada.

https://doi.org/10.1016/j.micres.2020.126426
Received 8 November 2019; Received in revised form 30 January 2020; Accepted 30 January 2020
Available online 07 February 2020
0944-5013/

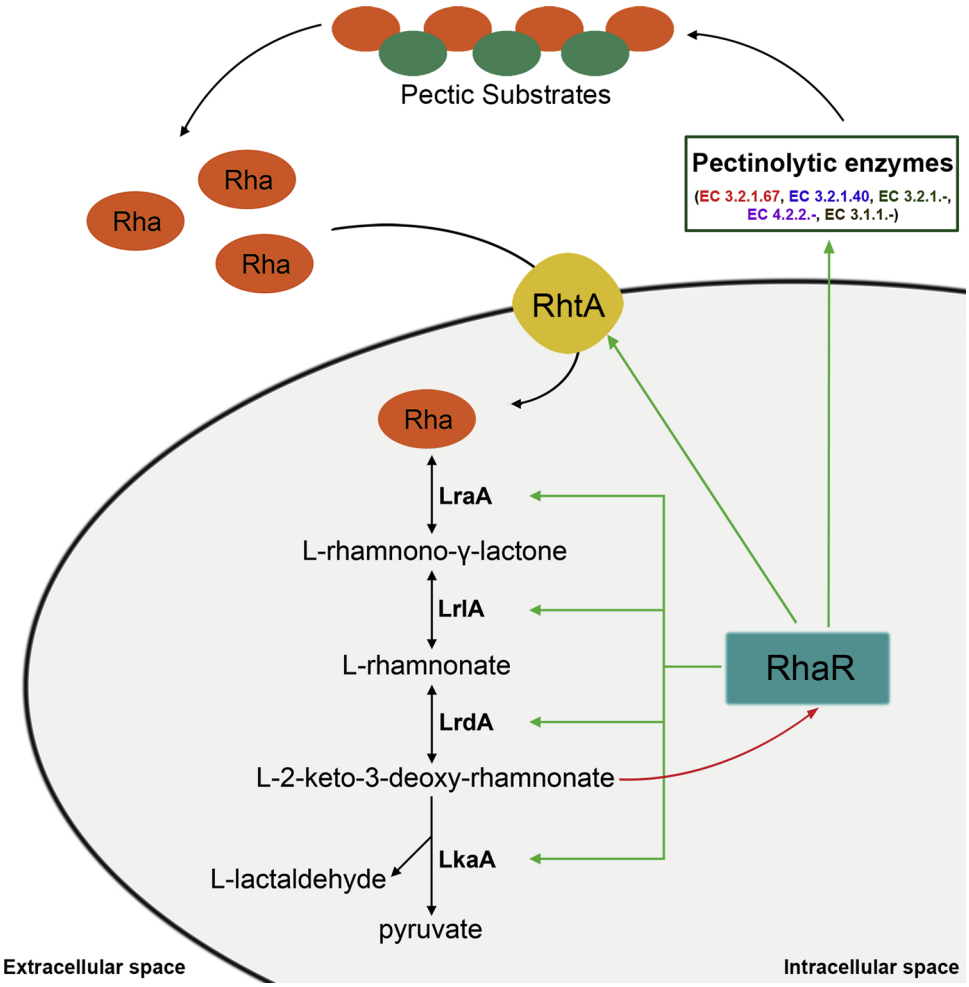

Fig. 1. Graphical representation of the L-rhamnose (Rha) catabolism and transcriptional regulation of the Rha-responsive genes in*A. niger*. The pathway regulator RhaR, which is activated by L-2-keto-3-deoxy-rhamnonate (red arrow), induces the genes required for the degradation of pectin and release of Rha, transport of Rha intracellularly and Rha catabolism (green arrows). LraA = L-rhamnose-1-dehydrogenase, LrlA = L-rhamnono-γ-lactonase, LrdA = L-rhamnonate dehydratase, LkaA = L-2-keto-3-deoxyrhamnonate (L-KDR) aldolase.

dehydratase (LrdA, formerly LraC; EC 4.2.1.65) and L-2-keto-3-deoxyrhamnonate (L-KDR) aldolase (LkaA; EC 4.1.2.53) (Watanabe et al., 2008). In *A. niger*, the genes involved in the first three enzymatic steps of this pathway have been identified and characterized (Khosravi et al., 2017). However, the gene(s) involved in the last conversion step of the pathway remains unknown. Previously, a bidirectional BlastP analysis against the *Aspergillus* genome database (www.aspgd.org/) showed that NRRL3_08779 is the closest *A. niger* homolog of *Scheffersomyces stipitis* Lra4 (Gruben et al., 2014). However, this gene was not expressed on Rha and its expression was not controlled by RhaR (Khosravi et al., 2017). Therefore, the involvement of three other putative genes, NRRL3_03899, NRRL3_05649 and NNRL3_06731, identified based on their InterPro and PFAM domain similarity to those found in Lra4 of *S. stipitis*, was assessed (Khosravi et al., 2017). In that case, all three genes were shown to be specifically upregulated in Rha, nevertheless, their deletion did not affect growth when Rha was used as sole carbon source, showing that they are not involved in Rha metabolism in *A. niger*.

We have renamed the genes of the Rha catabolic pathway, as our recent results clearly indicate that multiple genes/enzymes may be involved in several of the steps. According to common practice in *Aspergillus* gene/enzyme naming, genes are referred to by a 3-letter code, reflecting their function, followed by a letter, indicating the isogenes. The previously used names for the Rha pathway genes (*lraA*, *lraB* and *lraC*) do not follow this structure, as they encode different enzymatic functions, but have the same three-letter code. The use of the same code for different enzymes prevents the use of this code for isogenes encoding enzymes with similar activity. The new names suggested in this paper, provide a different three-letter code for each enzyme activity, as well as the option for referring to their corresponding iso-genes by the capital letter behind it.

Induction of the genes required for the degradation of pectin and release of Rha, transport of Rha into the cell and Rha catabolism, have been previously shown to be under control of the transcriptional regulator RhaR in *A. niger* (Gruben et al., 2014; Sloothaak et al., 2016; Gruben et al., 2017; Khosravi et al., 2017). The deletion of *rhaR*

Table 1
A. niger strains used in this study.

Strains	Formerly known as	Gene ID	Description	CBS number	Genotype	Reference
Reference strain (N593 Δ*kusA*)	–	–	–	CBS 138852	*A. niger* N593, *cspA1*, *kusA::amdS*, *pyrG*$^-$	(Meyer et al., 2007)
Δ*lraA*	Δ*lraA*	NRRL3_01494	L-rhamnose-1-dehydrogenase	CBS 144623	*A. niger* N593, *cspA1*, *kusA::amdS*, *pyrG*-, ***lraA-***	This study
Δ*lrlA*	Δ*lraB*	NRRL3_01493	L-rhamnono-γ-lactonase	CBS 144300	*A. niger* N593, *cspA1*, *kusA::amdS*, *pyrG*-, ***lrlA-***	This study
Δ*lrdA*	Δ*lraC*	NRRL3_01495	L-rhamnonate dehydratase	CBS 144313	*A. niger* N593, *cspA1*, *kusA::amdS*, *pyrG*-, ***lrdA-***	This study
Δ*lkaA*	Δ*lraD*	NRRL3_08604	L-2-keto-3-deoxyrhamnonate aldolase	CBS 144626	*A. niger* N593, *cspA1*, *kusA::amdS*, *pyrG*-, ***lkaA-***	This study
Δ*03333*	–	NRRL3_03333	putative L-2-keto-3-deoxyrhamnonate aldolase	CBS 145852	*A. niger* N593, *cspA1*, *kusA::amdS*, *pyrG*-, ***03333-***	This study
Δ*lkaA*Δ*03333*	–	NRRL3_08604 NRRL3_03333	–	CBS 145938	*A. niger* N593, *cspA1*, *kusA::amdS*, *pyrG*-, ***lkaA-, 03333-***	This study

resulted in strong reduction in expression of the catabolic pathway genes *lraA*, *lrlA* and *lrdA*, the Rha transporter gene *rhtA* (Sloothaak et al., 2016), as well as several Rha-releasing enzymes, during growth on both Rha and L-rhamnonate. The presence of Rha, even in low concentrations, has been shown to specifically induce the expression of *rhaR* (Sloothaak et al., 2016). Khosravi et al. (2017) showed that single gene deletions of *lraA*, *lrlA* and *lrdA* abolished induced expression of the RhaR-related genes, suggesting that the inducer of this regulator is further downstream in the pathway.

In this study, identification of the *lkaA* gene that is involved in the last step of Rha catabolism in *A. niger* showed that L-2-keto-3-deoxyrhamnonate is the inducer of the RhaR regulator. In particular, deletion of *lkaA* and transcriptomic analysis showed that the induction of the Rha pathway genes, the RhaR-regulated pectinolytic genes and *rhtA* in the Δ*lkaA* strain was maintained at similar levels as the reference strain.

2. Material and methods

2.1. Strains, media and growth conditions

The uridine auxotrophic and non-homologous end-joining (NHEJ) deficient *A. niger strain* N593Δ*kusA* (reference strain) was used as parental strain for the construction of the Δ*lraA*, Δ*lrlA*, Δ*lrdA*, Δ*lkaA* and Δ03333 mutants. For the double Δ*lkaA*Δ03333 mutant, the Δ*lkaA* strain was used as parental strain. All strains described in this study were deposited in the CBS strain collection of the Westerdijk Fungal Biodiversity Institute under accession numbers listed in Table 1. All strains were grown at 30 °C using Minimal Medium (MM, pH 6) or Complete Medium (CM, pH 6) with the appropriate carbon source (de Vries et al., 2004). For solid cultivation, 1.5 % (w/v) agar was added in the medium and, unless stated otherwise, all agar plates contained 1 % D-glucose as carbon source. As required, media of auxotrophic strains were supplemented with 1.22 g/L uridine, while a final concentration of 1.3 mg/mL of 5-fluoroorotic acid (5-FOA) was used for counter-selection of strains carrying the *pyrG* marker gene on the self-replicating plasmid.

For growth profiling, 6 cm petri dishes with vents containing MM agar supplemented with 25 mM D-glucose Sigma, G8270 or Rha Sigma, 83,650 were used. Spores were harvested from CM agar plates in ACES buffer, after five days of growth, and counted using a haemocytometer. Growth profiling plates were inoculated with 1000 spores in 2 µL, and incubated at 30 °C for 5 days. All liquid cultures were incubated in an orbital shaker at 250 rpm and 30 °C. For transfer experiments, the pre-cultures containing 250 ml CM with 2 % D-fructose in 1 L Erlenmeyer flasks were inoculated with 10^6 spores/mL and incubated for 16 h. Thereafter, the mycelia were harvested by filtration on sterile cheesecloth, washed with MM and ~0.5 g (dry weight) was transferred to 50 ml Erlenmeyer flasks containing 10 ml MM supplemented with 25 mM Rha. All cultures were performed in triplicate. After 2 h of incubation, the mycelia were harvested by vacuum filtration, dried between tissue paper and frozen in liquid nitrogen. Samples were stored at −80 °C.

2.2. Identification of candidate genes

Pathway hole filler (Green and Karp, 2004) from Pathway Tools software (Karp et al., 2016) was used to identify missing enzymes in the manually curated *A. niger* carbon metabolic network (Aguilar-Pontes et al., 2018) based on *A. niger* NRRL3 genome (Vesth et al., 2018; Aguilar-Pontes et al., 2018). Sequences for enzymes catalyzing the last step of the Rha pathway associated to EC 4.1.2.53 (2-keto-3-deoxy-L-rhamnonate aldolase) function were retrieved from Swiss-Prot (Boutet et al., 2016), MetaCyc PGDB (Caspi et al., 2016), including *Candida albicans* SC5314 and *Saccharomyces cerevisiae* PGDB YeastCyc (Karp et al., 2019). Their amino acid sequences were then used as queries in a BLASTP search against *A. niger* NRRL3 full proteome with the default E-

Table 2
Expression levels (FPKM) of putative *lkaA* genes in *A. niger* reference (Ref) and Δ*rhaR* strains, after their transfer for 2 h in liquid MM with 25 mM Rha or 25 mM D-glucose. The values are averages of duplicates. Fold changes > 1.5 and < 0.67 are highlighted in green and yellow, respectively, and padj_values < 0.05 are indicated with an asterisk (*). Genes selected for further analysis are underlined.

			RNA-sequencing This study			Microarray [a] Gruben *et al.* (2017)				
A. niger **NRRL3 model ID**	***A. niger*** **CBS 513.88 model ID**	**Gene**	**Mean Ref Glc**	**Mean Ref Rha**	**Fold change Ref Rha / Ref Glc**	**Mean Ref Glc**	**Mean Ref Rha**	**Mean Δ*rhaR* Rha**	**Fold change Ref Rha / Ref Glc**	**Fold change Δ*rhaR* Rha / Ref Rha**
NRRL3_08604	An03g02490	*lkaA*	39.7	1591.9	40.1 *	306.7	8462.1	849.8	27.6 *	0.1 *
NRRL3_03333	An12g05070		16.5	16.5	1.0	44.2	103.8	79.3	2.4 *	0.8 *
NRRL3_00191	An09g02440		0.1	0.5	8.7 *	21.8	26.7	19.0	1.2	0.7 *
NRRL3_09072	An12g01610		0,0	0.1	5.4	26.7	28.6	29.7	1.1	1.0
NRRL3_06259 [b]	-		1.0	0.9	0.9	-	-	-	-	-

[a] Based on the microarray dataset generated by Gruben et al. (2017).
[b] Expression data for NRRL3_06259 were not available in the microarray dataset generated by Gruben et al. (2017). Since this gene was lowly expressed (FPKM < 50) in our RNA-seq data, it was excluded for further analysis.

value cutoff of 10. Each of the candidate hits in the BLASTP results are evaluated by calculating the probability that the sequence encodes the desired function based on operon-, homology- and pathway-based data using the Bayesian network described in (Green and Karp, 2004). No hits were identified using the default probability-score of 0.9, however, 5 candidate hits were identified with a probability-score cutoff of 0.75 (Table 2).

2.3. Protoplast-mediated transformation, mutant purification and screening

For creation of all the mutants described in this study, the CRISPR/Cas9 system, as designed by (Song et al., 2018), was used. The Geneious R11 software (Kearse et al., 2012) was used for the identification of 20 bp guide sequences for our target genes against the *A. niger* NRRL3 genome. The guide sequences and plasmids used in this study are listed in Table A1.

To construct linear deletion DNA cassettes, the upstream and downstream flanking regions of the genes *lraA*, *lrlA*, *lrdA*, *lkaA* and 03333 were amplified by PCR using gene specific primers (see Table A2). PCR amplification was performed using Phusion™ High-Fidelity DNA Polymerase (Thermo Fisher Scientific), following manufacturer's instructions. Genomic DNA from reference strain was used as a template. The upstream reverse and the downstream forward primers were designed to harbor a barcode sequence [actgctaggattcgctatcg]. This sequence was used as the homologous region for the fusion of these two fragments in a PCR reaction, to generate the linear deletion DNA cassette. The amplified deletion cassettes were purified using the illustra GFX PCR DNA and Gel Band Purification Kit (GE Healthcare Life Sciences).

A. niger protoplasting was performed as described by (Kusters-van Someren et al., 1991) with some modifications. In particular, young mycelia from overnight culture were harvested by vacuum filtration, washed with 0.6 M $MgSO_4$ and dried between two tissue paper sheets. Mycelia were then incubated with VinoTaste® Pro lysing enzyme (0.75 g/gDW mycelia), dissolved in PS buffer (0.8 M sorbitol, 0.2 M sodium phosphate buffer pH 7.5), in an orbital shaker at 100 rpm and 34 °C. When free protoplasts were abundantly present (after ~2.5 h), mycelial debris was removed by filtration through Miracloth and protoplasts were collected by centrifugation (10 min, 3000 rpm, 4 °C). Protoplasts were then washed twice with ice-cold SC solution (1 M sorbitol, 50 mM $CaCl_2$*$2H_2O$) and resuspended in that buffer at an approximate concentration of $2*10^7$ protoplasts/ml. Transformation of *A. niger* protoplasts was performed as described in detail by (Kowalczyk et al., 2017).

All transformations were carried out using 0.8 μg of ANEp8-Cas9-gRNA plasmid DNA together with 4 − 6 μg of purified linear deletion DNA cassette. Since the reference strain is NHEJ-deficient, construction of mutants using a rescue cassette resulted in clean deletions. Transformants were plated on MM plates with 0.95 M sucrose. Five colonies per mutant were randomly selected from the transformation plates and streak-purified twice on MM plates. For *A. niger* colony PCR, genomic template DNA was isolated from mycelia of putative deletion strains using the Wizard® Genomic DNA Purification Kit (Promega). Correct mutants were identified by PCR amplification of the sequences flanking the CRISPR/Cas9 cut site, using primers listed in Table 4. Prior to storage, mutants were re-inoculated twice on MM plates supplemented with 1 % D-glucose and uridine, and subsequently on plates with 5-FOA aiming on counterselection against the ANEp8-Cas9-gRNA plasmids.

2.4. Transcriptome sequencing and analysis

The transcriptomic response of Δ*lkaA* induced after 2 h on Rha was analyzed using RNA-seq analysis. Total RNA was extracted from grinded mycelial samples using TRIzol® reagent (Invitrogen, Breda, The Netherlands) and purified with the NucleoSpin® RNA Clean-up Kit (Macherey-Nagel), while contaminant gDNA was removed by rDNase treatment directly on the silica membrane. The RNA quality and

Table 3
RNA-seq analysis of Rha-responsive genes, involved in (a) Rha catabolism, (b) transport of Rha intracellularly and (c) degradation of pectin and release of Rha, in *A. niger* Δ*lkaA* and the reference strains. For both strains, expression levels (FPKM) were measured after their transfer for 2 h in MM with 25 mM Rha. Genes with FPKM values < 50 are considered lowly expressed and marked in red font. The values are averages of duplicates. The fold change is the difference between the deletion mutants and the reference strain. Fold changes > 1.5 and < 0.67 are highlighted in green and red, respectively, and padj_values < 0.05 are indicated with an asterisk (*). [a] based on Khosravi et al. (2017). [b] based on Sloothaak et al. (2016).

				RNA-sequencing						
				This study						
		A. niger NRRL 3 model ID	Gene	mean Δ*lkaA*_Rha	mean Ref_Rha	fold change Δ*lkaA*/Ref	fold change Δ*lraA*/ Ref	fold change Δ*lrlA*/ Ref	fold change Δ*lrdA*/ Ref	fold change Δ*rhaR*/ Ref
a	Regulator	NRRL3_01496	*rhaR*	148,08	178,20	0,83 *	0,51 *	0,64 *	0,02 *	0,01 *
	L-rhamnose catabolic pathway genes	NRRL3_01494	*lraA*	2346,96	1813,98	1,29 *	0,00 *	0,13 *	0,17 *	0,04 *
		NRRL3_01493	*lrlA*	753,78	571,30	1,32 *	0,5 *	0,01 *	0,54 *	0,3 *
		NRRL3_01495	*lrdA*	13031,16	11841,31	1,10 *	0,09 *	0,13 *	0,00 *	0,00 *
		NRRL3_08604	*lkaA*	27,23	1591,85	0,02 *	0,08 *	0,1 *	0,27 *	0,16 *
b	L-rhamnose transporter genes	NRRL3_03278	*rhtA*	1275,54	936,98	1,36 *	0,19 *	0,30 *	0,00 *	0,01 *
		NRRL3_09860		1522,69	1337,17	1,14 *	0,06 *	0,08 *	0,05 *	0,05 *
		NRRL3_02828		1286,80	1438,45	0,89	0,14 *	0,19 *	0,01 *	0,01 *
		NRRL3_03147		1097,04	1306,42	0,84 *	1,40	1,94 *	1,61 *	1,08
		NRRL3_10300		262,18	307,30	0,85 *	1,44	1,69 *	2,13 *	3,27 *
		NRRL3_01652		190,52	73,62	2,59 *	2,34 *	1,56	1,23	0,77 *
		NRRL3_06137		5,96	4,84	1,23	0,63	0,37	0,39	3,46
		NRRL3_00235		7,93	4,59	1,73 *	1,97 *	1,16	1,52	6,81 *
c	CAZy under RhaR regulation	NRRL3_02832	*rgxA*	694,08	547,63	0,79 *	0,03 *	0,07 *	0,02 *	0,02 *
		NRRL3_08631	*rgxB*	109,66	139,27	1,27 *	0,01 *	0,04 *	0,00 *	0,00 *
		NRRL3_10559	*rgxC*	8,34	15,53	1,86 *	0,06 *	0,13 *	0,06 *	0,08 *
		NRRL3_02162		5437,00	3717,68	0,68 *	0,04 *	0,09 *	0,02 *	0,01 *
		NRRL3_06304		104,70	119,24	1,14 *	0,03 *	0,05 *	0,02 *	0,02 *
		NRRL3_03279		1009,92	1098,73	1,09	0,19 *	0,26 *	0,01 *	0,01 *
		NRRL3_04245		50,89	43,74	0,86 *	0,01 *	0,01 *	0,01 *	0,01 *
		NRRL3_07520		429,93	485,94	1,13 *	0,1 *	0,22 *	0,04 *	0,04 *
		NRRL3_00839	*urhgA*	4032,51	4531,18	1,12 *	0,08 *	0,12 *	0,02 *	0,02 *
		NRRL3_10115	*rglB*	2632,37	3144,23	1,19 *	0,03 *	0,07 *	0,00 *	0,01 *
		NRRL3_00169	*rgaeA*	207,88	233,14	1,12	0,27 *	0,26 *	0,08 *	0,06 *
		NRRL3_07501	*rgaeB*	569,31	535,23	0,94	0,19 *	0,21 *	0,06 *	0,05 *
		NRRL3_11738	*lacC*	178,79	228,08	1,28 *	0,07 *	0,16 *	0,03 *	0,05 *
		NRRL3_01071	*lacE*	9,76	17,88	1,83 *	0,12 *	0,10 *	0,21 *	0,18 *
		NRRL3_02931	*faeB*	28,23	19,30	0,68 *	0,33 *	0,27 *	0,28 *	0,25 *
		NRRL3_02827		45,97	35,42	0,77 *	0,07 *	0,06 *	0,02 *	0,03 *

quantity were analyzed with a RNA6000 Nano Assay using the Agilent 2100 Bioanalyzer (Agilent Technologies, Santa Clara, CA, USA). Purification of mRNA, synthesis of cDNA library and sequencing were conducted at DOE Joint Genome Institute (JGI).

RNA sample preparation was performed on the PerkinElmer Sciclone NGS robotic liquid handling system using the Illumina TruSeq Stranded mRNA HT sample prep kit, utilizing poly-A selection of mRNA following the protocol outlined by Illumina: https://support.illumina.com/sequencing/sequencing_kits/truseq-stranded-mrna.html, and with the following conditions: total RNA starting material was 1 μg per sample and eight cycles of PCR was used for library amplification. The prepared libraries were quantified using KAPA Biosystem's next-generation sequencing library qPCR kit and run on a Roche LightCycler 480 real-time PCR instrument. The quantified libraries were then

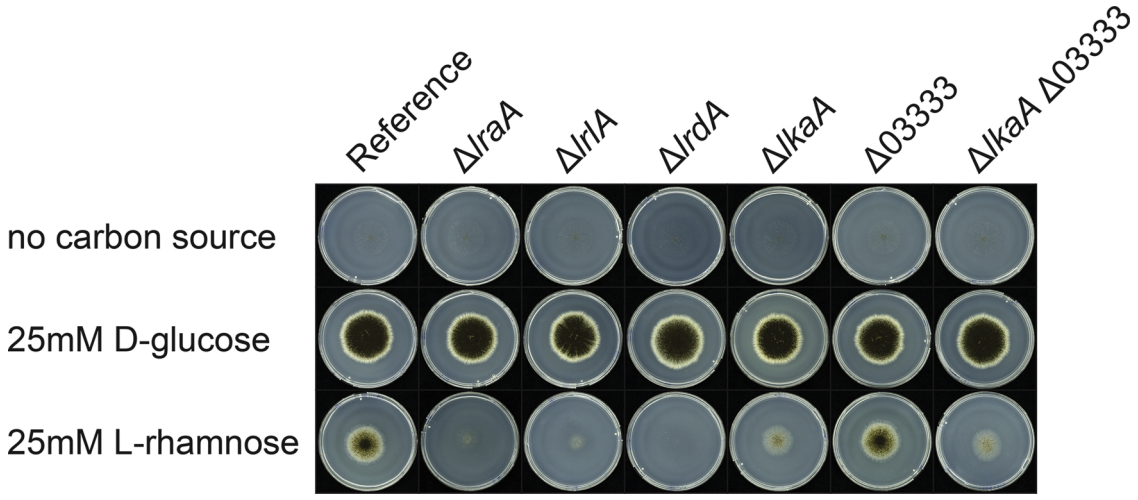

Fig. 2. Growth profiles of the reference strain (N593 Δ*kusA*) and the deletion mutants, Δ*lraA*, Δ*lrlA*, Δ*lrdA*, Δ*lkaA*, Δ03333 and Δ*lkaA*Δ03333, on solid MM without any carbon source, with 25 mM L-rhamnose or with 25 mM D-glucose. Strains were grown for 5 days at 30 °C.

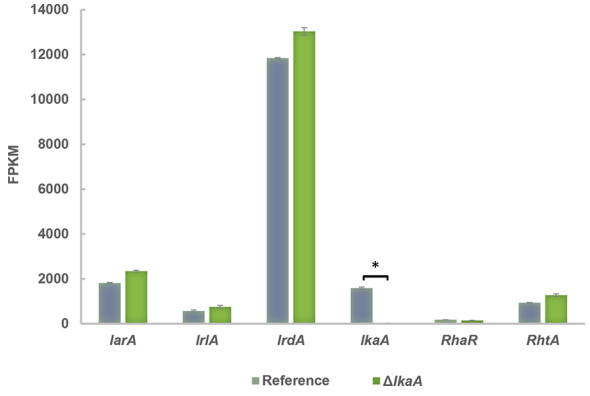

Fig. 3. Comparison of *A. niger lraA*, *lrlA*, *lrdA*, *lkaA*, *rhaR* and *rhtA* expression levels (FPKM) between the reference and the Δ*lkaA* strains. The expression was measured after transferring both strains for 2 h on 25 mM Rha. The expression levels represent mean values of triplicate samples. The cut-off for differential expression is DESeq2 fold change > 1.5 or < 0.67 and padj_value < 0.05. Significant differences in gene expression between these two strains are highlighted with an asterisk (*).

multiplexed with other libraries, and the pool of libraries was then prepared for sequencing on the Illumina NovaSeq sequencer using NovaSeq XP V1 reagent kits, S4 flow cell, and following a 2 × 150 indexed run recipe.

Using BBDuk (https://sourceforge.net/projects/bbmap), raw reads were evaluated for artifact sequence by kmer matching (kmer = 25), allowing one mismatch and detected artifact was trimmed from the 3′ end of the reads. RNA spike-in reads, PhiX reads and reads containing any Ns were removed. Quality trimming was performed using the phred trimming method set at Q6. Finally, following trimming, reads under the length threshold were removed (minimum length 25 bases or one third of the original read length – whichever was longer). Filtered reads from each library were aligned to the *A. niger* NRRL 3 (http://genome.jgi.doe.gov/Aspni_NRRL3_1) genome assembly using HISAT2 version 2.1.0 (Kim et al., 2015). FeatureCounts (Liao et al., 2014) was used to generate the raw gene counts using gff3 annotations. Only primary hits assigned to the reverse strand were included in the raw gene counts (-s 2 -p –primary options). The reads from each of the RNAseq samples were deposited with the Sequence Read Archive at NCBI with individual sample accession numbers (SRP225871, SRP225872, SRP226530, SRP226531 and SRP226532)

Statistical analysis was performed using DESeq2 (Love et al., 2014). Transcripts were considered differentially expressed if the DESeq2 fold change was > 1.5 or < 0.67 and Padj < 0.05 as well as the FPKM > 50 in at least one of the two conditions being compared. Transcripts with FPKM ≤ 50 were considered lowly (*i.e.* not substantially) expressed.

3. Results & discussion

3.1. Deletion of lkaA results in reduced growth on Rha

Candidate genes for the last step of the *A. niger* Rha catabolic pathway were identified as indicated in Materials and Methods. All of the candidates contained an HpcH/HpaI aldolase/citrate lyase domain (IPR005000, PF03328) according to InterPro (Mitchell et al., 2019) and PFAM (El-Gebali et al., 2019) database. This domain is also found in a number of proteins, including 2-keto-3-deoxy-L-rhamnonate aldolase (EC:4.1.2.53), 5-keto-4-deoxy-D-glucarate aldolase (EC:4.1.2.20) and citrate lyase subunit beta (EC:4.1.3.6).

Comparison of the expression levels of these five candidate genes on Rha and D-glucose (Table 2) showed that only the expression of NRRL3_08604, referred to from now on as *lkaA*, was significantly upregulated (40-fold) on Rha compared to D-glucose. However, analysis of the microarray data generated by Gruben et al. (2017) revealed that the expression of NRRL3_03333 was also induced (2.4-fold upregulated) on Rha compared to D-glucose. Therefore, both of these genes were selected for further analysis. The other three putative genes were either not induced by Rha or not expressed on either sugar in both datasets,

and were therefore excluded as candidates. Neither *lkaA* nor NRRL3_03333 were homologues of *S. stipitis* Lra4, nor did they belong to the same aldolase families as the previously described putative *lkaA* genes (see Table A3).

The *lkaA* gene was the only candidate that was strongly upregulated on Rha compared to D-glucose, which was regulated by RhaR (Table 2). Additionally, expression of *lkaA* was reduced in all three Δ*lraA*, Δ*lrlA* and Δ*lrdA* Rha metabolic mutants compared to the reference strain (Table 3). Deletion of *lkaA* resulted in reduced growth and sporulation on Rha as sole carbon source, which clearly showed that this gene is involved in the Rha catabolic pathway (Fig. 2). However, the residual growth on Rha suggests that the Δ*lkaA* mutant is still able to metabolize this sugar. Deletion of the NRRL3_03333 alone or in combination with Δ*lkaA* did not affect growth on Rha, indicating that this gene is not a paralog of *lkaA*.

3.2. Deletion of lkaA does not affect induction of RhaR regulated genes

As mentioned earlier, RhaR is activated in the presence of Rha. However, deletion of *lraA* resulted in inactivation of RhaR-mediated expression (Khosravi et al., 2017), which showed that Rha is not the actual inducer. Similarly, deletion of *lrlA* and *lrdA* also inactivated RhaR-mediated expression, demonstrating that neither L-rhamnono-γ-lactonase nor L-rhamnonate are inducers of RhaR.

This suggested that the inducer is located further down in the Rha catabolic pathway, and therefore the expression of the Rha-responsive genes that are under control of RhaR was also examined in the *lkaA* deletion mutant. The reference and the Δ*lkaA* strains were transferred to MM medium with 25 mM Rha, followed by RNA-seq analysis. The expression of *lkaA* in the Δ*lkaA* strain compared to reference strain was abolished, confirming the deletion of this gene. However, the expression levels of *lraA, lrlA*, *lrdA* and of the pathway regulator *rhaR* were the same as for the reference strain (Fig. 3; Table 3a), demonstrating that deletion of *lkaA* did not abolish activation of RhaR. This result was confirmed by qPCR analysis (data not shown).

The expression level of the *rhtA* Rha transporter followed the same pattern (Table 3b). Interestingly, two other putative transporter genes (NRRL3_09860 and NRRL3_02828) showed a similar expression profile, suggesting their involvement in Rha transport. While both genes were significantly downregulated in the Δ*lraA*, Δ*lrlA*, Δ*lrdA and* Δ*rhaR* mutants (Khosravi et al., 2017), their expression in the Δ*lkaA* mutant was similar to the reference strain. The same was observed for a third putative transporter gene (NRRL3_06137), but its expression levels were very low compared to *rhtA* and the other two candidate Rha transporter genes.

Finally, the expression of CAZy genes, previously shown to be regulated by RhaR (Gruben et al., 2017), was also compared between the *lkaA* deletion mutant and the reference strain. Several pectinolytic genes involved in the degradation of the RG-I backbone had similar expression levels in Δ*lkaA* and the reference strain. These included two GH28 exo-rhamnogalacturonases (*rgxA* and *rgxB*), five putative GH78 a-L-rhamnosidases (NRRL3_02162, NRRL3_06304, NRRL3_03279, NRRL3_04245 and NRRL3_07520), one GH105 unsaturated rhamnogalacturonan hydrolase (*urhgA*), one PL4 rhamnogalacturonan lyase (*rglB*) and two CE12 rhamnogalacturonan acetyl esterase (*rgaeA* and *rgaeB*) (Table 3c). A similar pattern was also observed for a gene (*lacC*) encoding a GH35 β-1,4-galactosidase acting on the pectic side chains. Previously, these genes were reported to be significantly (> 1.5 fold) down-regulated in all Δ*lraA*, Δ*lrlA*, Δ*lrdA and* Δ*rhaR* mutants compared to the reference strain on Rha (Khosravi et al., 2017).

Similar situation was also described for the GalUA catabolic pathway of *A. niger* (Alazi et al., 2017). In this pathway, which actually shares similarities regarding the conversion reactions of the pathway intermediates with the Rha catabolic pathway, deletion of *gaaC* led to the identification of 2-keto-3-deoxy-L-galactonate as the inducer of the transcriptional regulator GaaR. In particular, accumulation of 2-keto-3-deoxy-L-galactonate caused induction of the genes involved in pectin degradation, GalUA transport and GalUA catabolism.

4. Conclusions

Our results clearly demonstrate that in the Δ*lkaA* mutant the actual inducer of the RhaR regulator is still present. Since LkaA catalyzes the conversion of L-KDR into pyruvate and L-lactaldehyde, we conclude that L-KDR is the responsible metabolite for the induction of the Rha-responsive genes in *A. niger*. As the products of L-KDR conversion, pyruvate and L-lactaldehyde, are part of central metabolism, L-KDR is also the last Rha-specific metabolite of this pathway.

Funding sources

TC was supported by a grant of the NWO ALWOP.233 to RPdV. The work conducted by the U.S. Department of Energy Joint Genome Institute, a DOE Office of Science User Facility, was supported by the Office of Science of the U.S. Department of Energy under Contract No. DE-AC02-05CH11231. The Academy of Finland grant no. 308284 to MRM is acknowledged.

CRediT authorship contribution statement

Tania Chroumpi: Investigation, Writing - original draft. **Maria Victoria Aguilar-Pontes:** Formal analysis, Data curation, Writing - original draft. **Mao Peng:** Formal analysis, Data curation, Writing - review & editing. **Mei Wang:** Investigation. **Anna Lipzen:** Formal analysis. **Vivian Ng:** Project administration. **Igor V. Grigoriev:** Supervision, Writing - review & editing. **Miia R. Mäkelä:** Writing - review & editing. **Ronald P. de Vries:** Conceptualization, Supervision, Writing - review & editing, Funding acquisition.

Acknowledgements

The ANEp8-Cas9 plasmid was kindly provided by Prof. Adrian Tsang (CSFG, Concordia University, QC, Canada).

Appendix A

.

Table A1
Plasmids used in this study.

Plasmid	Description	CRISPR guide sequence	Reference
ANEp8-Cas9	Extra-chromosomal *cas9* expressing plasmid	–	Song et al. (2018)
ANEp8-Cas9-gRNA (*lraA*)	ANEp8-Cas9 with gRNA targeting *lraA*	GTAGCCGTAAACCACCTCGG	This study
ANEp8-Cas9-gRNA (*lrlA*)	ANEp8-Cas9 with gRNA targeting *lrlA*	CATCTTTGTGGCCTTCCCCG	This study
ANEp8-Cas9-gRNA (*lrdA*)	ANEp8-Cas9 with gRNA targeting *lrdA*	ATGACCGTCGAAGTCATCCG	This study
ANEp8-Cas9-gRNA (*lkaA*)	ANEp8-Cas9 with gRNA targeting *lkaA*	GTCCTAGTAGACGCCGAGCA	This study
ANEp8-Cas9-gRNA (03333)	ANEp8-Cas9 with gRNA targeting NRRL3_03333	ACGCAATCTGTGCAGTACCA	This study

Table A2
Primers used in this study. The 20 bp guide RNA (gRNA) sequences designed for the deletion of our target genes are indicated in red font. The linker sequence is depicted in lowercase/ bold font.

Primer name	Sequence (5′ to 3′)	Used for
G119_01493_fw	CATCTTTGTGGCCTTCCCCGGTTTTAGAGCTAGAAATAGCAAG	construction of the gRNA (*lrlA*)
G119_01493_rev	CGGGGAAGGCCACAAAGATGGACGAGCTTACTCGTTTCG	construction of the gRNA (*lrlA*)
left_01493_fw	CCTGGCATGGTTCTGGTAATTGG	amplification of *lrlA* 5’ flank
left_01493_rev	**cgatagcgaatcctagcagt**TGGCATTGTCGTGGGTGTAG	amplification of *lrlA* 5’ flank
right_01493_fw	**actgctaggattcgctatcg**GTGTGTAATGTGGGTGGAGG	amplification of *lrlA* 3’ flank
right_01493_rev	GGTAACAATCCCACGAGAAGC	amplification of *lrlA* 3’ flank/ checking the presence or absence of the *lrlA*
01493_NEST_fw	ACGAGTCAGGAGGGTGCTTG	fusion of *lrlA* 5’ and 3’ flanks
01493_NEST_rev	CGACCATCAACCACAATCAAC	fusion of *lrlA* 5’ and 3’ flanks
G12_01494_fw	GTAGCCGTAAACCACCTCGGGTTTTAGAGCTAGAAATAGCAAG	construction of the gRNA (*lraA*)
G12_01494_rev	CCGAGGTGGTTTACGGCTACGACGAGCTTACTCGTTTCG	construction of the gRNA (*lraA*)
left_01494_fw	GACGGGACTAAGGGATTTGC	amplification of *lraA* 5’ flank
left_01494_rev	**cgatagcgaatcctagcagt**TGTGATGGGTTGATTGTGGTTG	amplification of *lraA* 5’ flank
right_01494_fw	**actgctaggattcgctatcg**CTGGAAGAGGCTGCTAATGTG	amplification of *lraA* 3’ flank
right_01494_rev	GACTCCCACATCCACCTCTTCC	amplification of *lraA* 3’ flank/ checking the presence or absence of the *lraA*
01494_NEST_fw	AGAGATACCAATGACCTGTTCG	fusion of *lraA* 5’ and 3’ flanks
01494_NEST_rev	ACCACCTCCATTCCCACATC	fusion of *lraA* 5’ and 3’ flanks
G121_01495_fw	ATGACCGTCGAAGTCATCCGGTTTTAGAGCTAGAAATAGCAAG	construction of the gRNA (*lrdA*)
G121_01495_rev	CGGATGACTTCGACGGTCATGACGAGCTTACTCGTTTCG	construction of the gRNA (*lrdA*)
left_01495_fw	CGAAGGACTGGTGATGGATGG	amplification of *lrdA* 5’ flank
left_01495_rev	**cgatagcgaatcctagcagt**ATGTTGGCAGTAGTTTAGCGGAG	amplification of *lrdA* 5’ flank
right _01495_fw	**actgctaggattcgctatcg**GCTTCAATTCTCACTCCTGC	amplification of *lrdA* 3’ flank
right _01495_rev	TCCACATCAGAGAGATCATCAC	amplification of *lrdA* 3’ flank/ checking the presence or absence of the *lrdA*
01495_NEST_fw	AGCCGTCTCTGATGGTGAGC	fusion of *lrdA* 5’ and 3’ flanks
01495_NEST_rev	CACATAACCACTCAACTCCTCAC	fusion of *lrdA* 5’ and 3’ flanks
G37_08604_fw	GTCCTAGTAGACGCCGAGCAGTTTTAGAGCTAGAAATAGCAAG	construction of the gRNA (*lkaA*)
G37_08604_rev	TGCTCGGCGTCTACTAGGACGACGAGCTTACTCGTTTCG	construction of the gRNA (*lkaA*)
left_08604_fw	CTTGCTACTATCGACAACACAGG	amplification of *lkaA* 5’ flank
left_08604_rev	**cgatagcgaatcctagcagt**GGAGATGATCCTGAGCGTGG	amplification of *lkaA* 5’ flank
right_08604_fw	**actgctaggattcgctatcg**GTTGAAGAGCGTTACGGAGG	amplification of *lkaA* 3’ flank
right_08604_rev	TGATTCCGTTAGTCGTTCTTCC	amplification of *lkaA* 3’ flank/ checking the presence or absence of the *lkaA*
08604_NEST_fw	AGTAGCACAGCCAACAAGAACG	fusion of *lkaA* 5’ and 3’ flanks
08604_NEST _rev	TGAGCAAATCAAGCAGAGAGAGG	fusion of *lkaA* 5’ and 3’ flanks
G53_03333_fw	ACGCAATCTGTGCAGTACCAGTTTTAGAGCTAGAAATAGCAAG	construction of the gRNA (03333)
G53_03333_rev	TGGTACTGCACAGATTGCGTGACGAGCTTACTCGTTTCG	construction of the gRNA (03333)
left_03333_fw	GGAGCAGCAATGGAAATGAAAC	amplification of NRRL3_03333 5′ flank
left_03333_rev	**cgatagcgaatcctagcagt**CGATCATAGGCAGGGTAGATTG	amplification of NRRL3_03333 5′ flank
right_03333_fw	**actgctaggattcgctatcg**GTGTCGGTAGTGTCAGGAGG	amplification of NRRL3_03333 3′ flank
right_03333_rev	TGTTGGAAGAGAAGCCGAGG	amplification of NRRL3_03333 3′ flank/ checking the presence or absence of the NRRL3_03333
03333_NEST_fw	ACCGAAGGTGGTTAGTTCATGC	fusion of NRRL3_03333 5′ and 3′ flanks
03333_ NEST _rev	TTGATGAATCCGCGAAGGATAGG	fusion of NRRL3_03333 5′ and 3′ flanks
linker_fw	ACTGCTAGGATTCGCTATCG	checking the presence or absence of the target genes

Table A3
Comparison of the domains in characterized L-2-keto-3-deoxyrhamnonate aldolase.

Strains	Gene ID	Annotation	InterProScan	Pfam	References
Scheffersomyces stipitis	PICST_64442	L-KDR aldolase	IPR002220:DapA-like | IPR013785:Aldolase-type TIM barrel	PF00701:Dihydrodipicolinate synthetase family	[a] (Koivistoinen et al., 2012)
Aspergillus niger NRRL3	NRRL3_03899	N-acetylneuraminate lyase	IPR002220:DapA-like | IPR013785:Aldolase-type TIM barrel	PF00701:Dihydrodipicolinate synthetase family	[b] (Khosravi et al., 2017)
	NRRL3_05649	N-acetylneuraminate lyase	IPR013785:Aldolase-type TIM barrel | IPR002220:DapA-like	PF00701:Dihydrodipicolinate synthetase family	[b] (Khosravi et al., 2017)
	NRRL3_06731	DapA-like protein	IPR013785:Aldolase-type TIM barrel | IPR002220:DapA-like	PF00701:Dihydrodipicolinate synthetase family	[b] (Khosravi et al., 2017)
	NRRL3_08604	HpcH/ HpaI aldolase/citrate lyase domain-containing protein	IPR005000: HpcH/HpaI aldolase/citrate lyase domain	PF03328: HpcH/HpaI aldolase/citrate lyase family	This study
	NRRL3_03333	HpcH/ HpaI aldolase/citrate lyase domain-containing protein	IPR005000: HpcH/HpaI aldolase/citrate lyase domain	PF03328: HpcH/HpaI aldolase/citrate lyase family	This study

[a]Koivistoinen, O.M., Arvas, M., Headman, J.R., Andberg, M., Penttilä, M., Jeffries, T.W., Richard, P., 2012. Characterisation of the gene cluster for L-rhamnose catabolism in the yeast *Scheffersomyces* (*Pichia*) *stipitis*. Gene 492, 177-85.
[b]Khosravi, C., Kun, R.S., Visser, J., Aguilar-Pontes, M.V., de Vries, R.P., Battaglia, E., 2017. *In vivo* functional analysis of L-rhamnose metabolic pathway in *Aspergillus niger*: A tool to identify the potential inducer of RhaR. BMC Microbiol. 17, 214.

Appendix B. Supplementary data

Supplementary material related to this article can be found, in the online version, at doi:https://doi.org/10.1016/j.micres.2020.126426.

References

Aguilar-Pontes, M.V., Brandl, J., McDonnell, E., Strasser, K., Nguyen, T.T.M., Riley, R., Mondo, S., Salamov, A., Nybo, J.L., Vesth, T.C., Grigoriev, I.V., Andersen, M.R., Tsang, A., de Vries, R.P., 2018. The gold-standard genome of *Aspergillus niger* NRRL 3 enables a detailed view of the diversity of sugar catabolism in fungi. Stud. Mycol. 91, 61–78.

Alazi, E., Khosravi, C., Homan, T.G., du Pré, S., Arentshorst, M., Di Falco, M., Pham, T.T.M., Peng, M., Aguilar-Pontes, M.V., Visser, J., Tsang, A., de Vries, R.P., Ram, A.F.J., 2017. The pathway intermediate 2-keto-3-deoxy-L-galactonate mediates the induction of genes involved in D-galacturonic acid utilization in *Aspergillus niger*. FEBS Lett. 591, 1408–1418.

Benoit, I., Coutinho, P.M., Schols, H.A., Gerlach, J.P., Henrissat, B., de Vries, R.P., 2012. Degradation of different pectins by fungi: correlations and contrasts between the pectinolytic enzyme sets identified in genomes and the growth on pectins of different origin. BMC Genomics 13, 321.

Boutet, E., Lieberherr, D., Tognolli, M., Schneider, M., Bansal, P., Bridge, A.J., Poux, S., Bougueleret, L., Xenarios, I., 2016. UniProtKB/Swiss-Prot, the manually annotated section of the UniProt KnowledgeBase: how to use the entry view. Methods Mol. Biol. 1374, 23–54.

Caspi, R., Billington, R., Ferrer, L., Foerster, H., Fulcher, C.A., Keseler, I.M., Kothari, A., Krummenacker, M., Latendresse, M., Mueller, L.A., Ong, Q., Paley, S., Subhraveti, P., Weaver, D.S., Karp, P.D., 2016. The MetaCyc database of metabolic pathways and enzymes and the BioCyc collection of pathway/genome databases. Nucleic Acids Res. 44, D471–480.

de Vries, R.P., Visser, J., 2001. *Aspergillus* enzymes involved in degradation of plant cell wall polysaccharides. Microbiol. Mol. Biol. Rev. 65, 497–522.

de Vries, R.P., Kester, H.C.M., Poulsen, C.H., Benen, J.A.E., Visser, J., 2000. Synergy between enzymes from *Aspergillus* involved in the degradation of plant cell wall polysaccharides. Carbohydr. Res. 327, 401–410.

de Vries, R.P., Burgers, K., van de Vondervoort, P.J.I., Frisvad, J.C., Samson, R.A., Visser, J., 2004. A new black *Aspergillus* species, *A. vadensis*, is a promising host for homologous and heterologous protein production. Appl. Environ. Microbiol. 70, 3954–3959.

El-Gebali, S., Mistry, J., Bateman, A., Eddy, S.R., Luciani, A., Potter, S.C., Qureshi, M., Richardson, L.J., Salazar, G.A., Smart, A., Sonnhammer, E.L.L., Hirsh, L., Paladin, L., Piovesan, D., Tosatto, S.C.E., Finn, R.D., 2019. The Pfam protein families database in 2019. Nucleic Acids Res. 47, D427–D432.

Green, M.L., Karp, P.D., 2004. A Bayesian method for identifying missing enzymes in predicted metabolic pathway databases. BMC Bioinformatics 5, 76.

Gruben, B., Zhou, M., Wiebenga, A., Ballering, J., Overkamp, K., Punt, P., Vries, R.P., 2014. *Aspergillus niger* Rhar, a regulator involved in L-rhamnose release and catabolism. Appl. Microbiol. Biotechnol. 98, 5531–5540.

Gruben, B.S., Mäkelä, M.R., Kowalczyk, J.E., Zhou, M., Benoit-Gelber, I., De Vries, R.P., 2017. Expression-based clustering of CAZyme-encoding genes of *Aspergillus niger*. BMC Genomics 18, 900.

Karp, P.D., Latendresse, M., Paley, S.M., Krummenacker, M., Ong, Q.D., Billington, R., Kothari, A., Weaver, D., Lee, T., Subhraveti, P., Spaulding, A., Fulcher, C., Keseler, I.M., Caspi, R., 2016. Pathway Tools version 19.0 update: software for pathway/genome informatics and systems biology. Brief. Bioinform. 17 (5), 877–890.

Karp, P.D., Billington, R., Caspi, R., Fulcher, C.A., Latendresse, M., Kothari, A., Keseler, I.M., Krummenacker, M., Midford, P.E., Ong, Q., Ong, W.K., Paley, S.M., Subhraveti, P., 2019. The BioCyc collection of microbial genomes and metabolic pathways. Brief. Bioinform. 20 (4), 1085–1093.

Kearse, M., Moir, R., Wilson, A., Stones-Havas, S., Cheung, M., Sturrock, S., Buxton, S., Cooper, A., Markowitz, S., Duran, C., Thierer, T., Ashton, B., Meintjes, P., Drummond, A., 2012. Geneious basic: An integrated and extendable desktop software platform for the organization and analysis of sequence data. Bioinformatics 28, 1647–1649.

Khosravi, C., Kun, R.S., Visser, J., Aguilar-Pontes, M.V., de Vries, R.P., Battaglia, E., 2017. *In vivo* functional analysis of L-rhamnose metabolic pathway in *Aspergillus niger*: a tool to identify the potential inducer of RhaR. BMC Microbiol. 17, 214.

Kim, D., Langmead, B., Salzberg, S.L., 2015. HISAT: a fast spliced aligner with low memory requirements. Nat. Meth. 12, 357–360.

Kowalczyk, J.E., Lubbers, R.J.M., Peng, M., Battaglia, E., Visser, J., de Vries, R.P., 2017. Combinatorial control of gene expression in *Aspergillus niger* grown on sugar beet pectin. Sci. Rep. 7, 12356.

Kusters-van Someren, M.A., Harmsen, J.A.M., Kester, H.C.M., Visser, J., 1991. Structure of the *Aspergillus niger pelA* gene and its expression in *Aspergillus niger* and *Aspergillus nidulans*. Curr. Genet. 20, 293–299.

Liao, Y., Smyth, G.K., Shi, W., 2014. featureCounts: an efficient general purpose program for assigning sequence reads to genomic features. Bioinformatics 30, 923–930.

Love, M.I., Huber, W., Anders, S., 2014. Moderated estimation of fold change and dispersion for RNA-seq data with DESeq2. Genome Biol. 15, 550.

Martens-Uzunova, E., Schaap, P., 2009. Assessment of the pectin degrading enzyme network of *Aspergillus niger* by functional genomics. Fungal Genet. Biol. 46, S170–S179.

Meyer, V., Arentshorst, M., El-Ghezal, A., Drews, A.-C., Kooistra, R., van den Hondel,

C.A.M.J.J., Ram, A.F.J., 2007. Highly efficient gene targeting in the *Aspergillus niger kusA* mutant. J. Biotechnol. 128, 770–775.

Mitchell, A.L., Attwood, T.K., Babbitt, P.C., Blum, M., Bork, P., Bridge, A., Brown, S.D., Chang, H.Y., El-Gebali, S., Fraser, M.I., Gough, J., Haft, D.R., Huang, H., Letunic, I., Lopez, R., Luciani, A., Madeira, F., Marchler-Bauer, A., Mi, H., Natale, D.A., Necci, M., Nuka, G., Orengo, C., Pandurangan, A.P., Paysan-Lafosse, T., Pesseat, S., Potter, S.C., Qureshi, M.A., Rawlings, N.D., Redaschi, N., Richardson, L.J., Rivoire, C., Salazar, G.A., Sangrador-Vegas, A., Sigrist, C.J.A., Sillitoe, I., Sutton, G.G., Thanki, N., Thomas, P.D., Tosatto, S.C.E., Yong, S.Y., Finn, R.D., 2019. InterPro in 2019: improving coverage, classification and access to protein sequence annotations. Nucleic Acids Res. 47, D351–360.

Sloothaak, J., Odoni, D.I., Martins Dos Santos, V.A., Schaap, P.J., Tamayo-Ramos, J.A., 2016. Identification of a novel L-rhamnose uptake transporter in the filamentous fungus *Aspergillus niger*. PLoS Genet. 12, e1006468.

Song, L., Ouedraogo, J.-P., Kolbusz, M., Nguyen, M., Tsang, A., 2018. Efficient genome editing using tRNA promoter-driven CRISPR/Cas9 gRNA in *Aspergillus niger*. PLoS One 13, e0202868.

Vesth, T.C., Nybo, J.L., Theobald, S., Frisvad, J.C., Larsen, T.O., Nielsen, K.F., Hoof, J.B., Brandl, J., Salamov, A., Riley, R., Gladden, J.M., Phatale, P., Nielsen, M.T., Lyhne, E.K., Kogle, M.E., Strasser, K., McDonnell, E., Barry, K., Clum, A., Chen, C., LaButti, K., Haridas, S., Nolan, M., Sandor, L., Kuo, A., Lipzen, A., Hainaut, M., Drula, E., Tsang, A., Magnuson, J.K., Henrissat, B., Wiebenga, A., Simmons, B.A., Mäkelä, M.R., de Vries, R.P., Grigoriev, I.V., Mortensen, U.H., Baker, S.E., Andersen, M.R., 2018. Investigation of inter- and intra-species variation through genome sequencing of *Aspergillus* section *Nigri*. Nat. Genet. 50 (12), 1688–1695.

Voragen, A.G.J., Coenen, G.-J., Verhoef, R.P., Schols, H.A., 2009. Pectin, a versatile polysaccharide present in plant cell walls. Struct. Chem. 20, 263.

Watanabe, S., Saimura, M., Makino, K., 2008. Eukaryotic and bacterial gene clusters related to an alternative pathway of nonphosphorylated L-rhamnose metabolism. J. Biol. Chem. 283, 20372–20382.